

1 **Response to Anonymous Referee #1**

2 We thank the reviewer for their comments and suggestions that have improved the
3 manuscript. Responses to their comments are in bold below.

4

5 1) I thought that the title was fine, but it could even be revised slightly if the authors choose to
6 in order to advertise the overall impact of their work even more since they go beyond just
7 reporting composition data in the paper.

8 - **The title has been changed to 'The impacts of aerosol loading, composition and water
9 uptake on aerosol extinction variability in the Baltimore-Washington, D.C. region'**

10 2) Major Comments: While this may be out of the scope of this study and up to the authors if
11 they want to address it, this reviewer is curious to know if anything can be said about the
12 impact of aqueous processing (i.e., cloud droplets, deliquesced aerosol) in influencing
13 aerosol composition in the study region.

14 - **We have included a discussion of the work by Eck et al (ACP, 2014) who utilized data
15 from DISCOVER-AQ to show large increases in AERONET-measured AOD (on average of
16 25%) in the vicinity of non-precipitating cumulus clouds in the region. In situ
17 measurements showed increases in aerosol scattering, volume and mass in spirals
18 measured before and after cloud formation. These included a doubling of water-
19 soluble organics and 50% increase in sulfate.**

20 3) Specific Comments: Page 23321, Line 8: Just to confirm, aerosol size distribution is not being
21 mentioned here because 'aerosol loading' incorporates the impact of varying size
22 distributions. Is this what the idea is here and throughout the paper?

23 - **Correct, aerosol loading is used to encapsulate any changes due to variability in aerosol
24 number, size and mass scattering efficiencies.**

25 4) Page 23323, Line 3: The r^2 value would mean more if authors report at least the sample
26 number or some kind of measure of the statistical significance of the correlation (i.e., what %
27 confidence?).

28 - **Done, the comparison between in situ and remote sensing extinction measurements
29 was based on 668 data points**

30 5) Section 2: In the discussion of the PILS measurements, a few more details are recommended:
31 a. (i) is PM1.0, PM2.5, or some other size range being sampled?;

32 - **The size range measured by the PILS was largely controlled by the size cut of
33 the inlet (4 micron) and the denuders. The transport efficiency of the PILS
34 integrated onto the P-3B was not fully studied but is believed to give a cut size
35 of somewhere between 1 and 2.5 microns. Measurements by an aerodynamic
36 particle sizer (0.5-20microns) showed that aerosol in the region was dominated
37 by sub-micron aerosol. A sentence has been added to the text.**

38 b. (ii) were denuders used for the measurements to avoid positive contamination from
39 VOCs and inorganic acids and bases?;

40 - **Yes, they were used and a sentence has been added to the text.**

41 c. (iii) the list of species in Line 7-8 on Page 23324 does not mention lithium and thus it
42 is uncertain as to how the dilution factor was estimated for the two PILS
43 instruments;

44 - **I did not mention this previously but LiBr was added to the water supply to
45 measure dilution. A sentence has been added to the text.**

1 d. (iv) no mention is made about the impact of volatilization in the PILS when discussing
2 the mass closure statistics around Line 19 of Page 23324. The readers should refer to
3 this possibility and reference the detailed results in previous work that showed that
4 on average, slightly more than 10% of the ammonium is lost in the PILS with a tip
5 temperature of approximately 100 C: Sorooshian, A., F. J. Brechtel, Y. L. Ma, R. J.
6 Weber, A. Corless, R. C. Flagan, and J. H. Seinfeld (2006). Modeling and
7 characterization of a particle-into-liquid sampler (PILS), Aerosol Sci. Tech., 40, 396-
8 409.

9 - **Done, thanks**

- 10 6) Page 23324, Lines 15-24: are the sizes sampled by the PILS and UHSAS the same?
11 - **The UHSAS measured 60nm to 1000 micron and thus not identical to the PILS.**
12 **However, measurements by an aerodynamic particle sizer (0.5-20microns) showed that**
13 **aerosol in the region was dominated by sub-micron aerosol.**
- 14 7) Page 23324, Lines 15-24: Another interesting piece of analysis that could shed light on the
15 18% of mass is a simple charge balance of the PILS species measured. It would be useful to
16 see just how well the closure is between anion and cation species charges.
17 - **Good closure (slope of 0.98 with an R2 of 0.94 for all samples) suggests that any loss**
18 **mechanisms are equivalent for anions and cations. A sentence relating this has been**
19 **added.**
- 20 8) Page 23325, Line 29: It would be interesting for the authors to refer to Table 6 of the
21 Sorooshian et al. paper noted above since the true ratio may have even been higher due to
22 the impact of volatilization on reducing this ratio in the PILS instrument.
23 - **done**
- 24 9) Page 23326, Lines 11-14 and other areas: when the authors refer to ‘ammonium sulfate’ and
25 ‘ammonium nitrate’, it is assumed that they have confirmed that the molar ratios of their
26 measurements agree with the expected 2.0 and 1.0 ratios for these species for each
27 individual flight that they refer to in such sentences. Since thermodynamically ammonium
28 has a preference to neutralize sulfate first, the excess ammonium needs to then be
29 compared to nitrate mass to confirm that a 1.0 ratio exists. More discussion about this issue
30 is warranted since this reviewer finds it too simple just to refer to ‘ammonium nitrate’ and
31 ‘ammonium sulfate’ without some more discussion of flight-byflight statistics of these molar
32 ratios.
33 - **The molar ratio of ammonium-to-sulfate varied between 1.9 and 2.3 on days with high**
34 **aerosol loadings suggesting on these days that the sulfate was fully neutralized. On**
35 **low loading days the ratio is more variable and uncertain. Thus it is not correct to refer**
36 **to them as ammonium sulfate. Nitrate was a very minor component and excess**
37 **ammonium and nitrate were not highly correlated except on flight 11 (which had the**
38 **highest nitrate) when the ratio was 1.15. Because of this uncertainty, wording**
39 **throughout the text has been shifted to sulfate and nitrate aerosol.**
- 40 10) Page 23333, Line 21: add units of ug/m3 to the aerosol concentration.
41 - **done**
- 42 11) Figure 4: Some of the species charges are incorrect. Authors should check these, especially
43 for calcium and magnesium.
44 - **done, thanks for catching this error!**

45

1 **Response to Anonymous Referee #2**

2 We thank the reviewer for their comments and suggestions that have improved the
3 manuscript. Responses to their comments are in bold below.

4

5 1) Page 23325, line 19. How do these altitude-limited AODs compare with the full-column AOD?
6 The latter, available from DRAGON AERONET sites (Eck et al., 2014 ACP), is more relevant to
7 satellite-based aerosol measurements and their variabilities (e.g., Munchak et al., 2013,
8 AMT).

9 - **A comparison between AOD based on in situ measurements (with vertical profiles
10 extended to ground level) and AERONET AOD is in preparation by co-author Luke
11 Ziemba. Good agreement is seen when AOD is above 0.4. Below 0.4, AERONET is higher
12 than in situ AOD by approximately 0.04. The causes of this will be studied in this future
13 manuscript and may include 1) aerosol above the aircraft, 2) a strong gradient in
14 aerosol at the ground level, 3) the hygroscopic treatment of aerosol, or 4) loss of large
15 aerosol (dust) in the aircraft inlet. The fairly good agreement is discussed in my revised
16 manuscript with a more exhaustive comparison left for Ziemba et al.**

17 2) Page 23325, line 29. The molar ratio of 1.92 is inconsistent with the numbers in the previous
18 sentence and the inference made in this sentence. If sulfate (96 g/mol) is 23% by mass and if
19 ammonium (18 g/mol) is 10%, the ratio must be $(23/96)/(10/18) = 0.43$. If sulfate is almost
20 completely neutralized as ammonium sulfate, the ratio must be ~ 0.5 or lower.

21 - **This was a typo and has been changed to a ratio of ammonium-to-sulfate of 1.92 (not
22 the reverse as was originally stated) which is near 2 signifying nearly neutralized
23 ammonium sulfate**

24 3) Page 23331, line 5. "3 to 4 values" – why is this greater than the number of circuits given in
25 Table 1?

26 - **Table 1 only includes full circuits (where all 6 sites were visited). At the end of some
27 flights, additional spirals were performed over select sites. Thus during a flight there
28 may have been 3 full circuits but 4 spirals could be performed at some of the sites. A
29 sentence discussing this has been added to the Mission Overview and the Diurnal
30 Variability sections and to the Table 1 caption.**

31 4) Page 23332, line 29. The ambient extinction estimated from the monthly average dry
32 extinction, shown in the right column of Figure 15, varies little. Does the calculation use the
33 observed, pre-averaging RH, gamma and SSA? If so, is the result consistent with, for example,
34 the top right panel of Figure 12 where the first two spirals of Flight 14, Site 4 saw similar dry
35 extinctions but different (by $\sim 15\%$) ambient extinctions?

36 - **The ambient extinction for each spiral site in the right column was based on the actual
37 observed pre-averaging RH, gamma and SSA, and the monthly average dry extinction.
38 The reason the percent biases are so large is because the dry extinction varies so much
39 from day-to-day (top of Fig. 15). The right panel of Fig. 12 shows an extreme case
40 where RH is important (causes about 50% of the variability in ambient extinction). In
41 Fig. 16 you can cause biases of up to 50% but this is small in comparison with the 400%
42 due to using monthly average dry extinction.**

43 5) Page 23333, line 11. Replace the semicolon with a comma.

44 - **done**

45 6) Page 23333, line 16. Replace "as such" with "as follows".

- 1 - **done**
- 2 7) Figure 5. Caption. "left" in the last pair of parentheses should read "right".
- 3 - **done**

4
5
6
7
8
9
10
11
12
13
14
15
16
17
18
19
20
21
22
23
24
25
26
27

1 **Response to Anonymous Referee #3**

2 We thank the reviewer for their comments and suggestions that have improved the
3 manuscript. Responses to their comments are in bold below.

4

5 1) Echoing one of the other reviewer comments, the title could be improved to better reflect
6 the actual nature of the paper.

7 - **The title has been changed to 'The impacts of aerosol loading, composition and water**
8 **uptake on aerosol extinction variability in the Baltimore-Washington, D.C. region'**

9 2) Pg. 23319, line 1: specify what is meant by 'aerosol loading' (mass loading, aerosol extinction.
10 . .)

11 - **done, dry extinction**

12 3) Pg. 23324, line 6-7: it is quite common, but provide basic details of ion chromatographic
13 analysis

14 - **done**

15 4) Pg. 23326, line 21: refer here to Equation 5

16 - **done**

17 5) Pg. 23327, line 13-16: Delete 'To a first approximation' and replace 'showing' with
18 'suggesting'

19 - **done**

20 6) Pg. 23331, line 18-19: I don't see this information conveyed in Fig. 11?

21 - **This refers to the highest orange marker seen in the right panel of Fig. 11. Text has**
22 **been added to this sentence to clarify**

23 7) Pg. 23319, line 2: ". . .for 88

24 - **We are not sure what is referred to here. Please clarify if needed.**

25 8) Pg. 23325, line 29: should be ammonium to sulfate molar ratio

26 - **done**

27 9) Pg. 23333, line 7: Brock et al., 2015 does not appear as a reference

28 - **added**

29

30

31

32

33

34

1 **The impacts of aerosol loading, composition and water**
2 **uptake on aerosol extinction variability in the Baltimore-**
3 **Washington, D.C. region**

Deleted: Aerosol composition and

4
5 **A. J. Beyersdorf¹, L. D. Ziemba¹, G. Chen¹, C. A. Corr^{1,2}, J. H. Crawford¹, G. S.**
6 **Diskin¹, R. H. Moore¹, K. L. Thornhill^{1,3}, E. L. Winstead^{1,3}, and B. E. Anderson¹**

7 [1]{NASA Langley Research Center, Hampton, Virginia}

8 [2]{Oak Ridge Associated Universities, Oak Ridge, Tennessee}

9 [3]{Science Systems and Applications, Inc., Hampton, Virginia}

10 Correspondence to: A. J. Beyersdorf (andreas.j.beyersdorf@nasa.gov)

11
12 **Abstract**

13 In order to utilize satellite-based aerosol measurements for the determination of air quality,
14 the relationship between aerosol optical properties (wavelength-dependent, column-integrated
15 extinction measured by satellites) and mass measurements of aerosol loading (PM_{2.5} used for
16 air quality monitoring) must be understood. This connection varies with many factors
17 including those specific to the aerosol type, such as composition, size and hygroscopicity, and
18 to the surrounding atmosphere, such as temperature, relative humidity (RH) and altitude, all
19 of which can vary spatially and temporally. During the DISCOVER-AQ (Deriving
20 Information on Surface conditions from Column and Vertically Resolved Observations
21 Relevant to Air Quality) project, extensive in-situ atmospheric profiling in the Baltimore, MD
22 – Washington, D.C. region was performed during fourteen flights in July 2011. Identical
23 flight plans and profile locations throughout the project provide meaningful statistics for
24 determining the variability in and correlations between aerosol loading, composition, optical
25 properties and meteorological conditions.

26 Measured water-soluble aerosol mass was composed primarily of ammonium sulfate
27 (campaign average of 32%) and organics (57%). A distinct difference in composition was
28 observed with high-loading days having a proportionally larger percentage of sulfate due to
29 transport from the Ohio River Valley. This composition shift caused a change in the aerosol

Deleted: ammonium

Deleted: (up to 49%)

1 water-uptake potential (hygroscopicity) such that higher relative contributions of inorganics
2 increased the bulk aerosol hygroscopicity. These days also tended to have higher relative
3 humidity causing an increase in the water content of the aerosol. Conversely, low aerosol
4 loading days had lower sulfate and higher black carbon contributions causing lower single
5 scattering albedos (SSAs). The average black carbon concentrations were 240 ng m⁻³ in the
6 lowest 1 km decreasing to 35 ng m⁻³ in the free troposphere (above 3 km).

Deleted: ammonium sulfate

Deleted: ammonium

7 Routine airborne sampling over six locations was used to evaluate the relative contributions
8 of aerosol loading, composition, and relative humidity (the amount of water available for
9 uptake onto aerosols) to variability in mixed layer aerosol extinction. Aerosol loading (dry
10 extinction) was found to be the predominant source accounting for 88% on average of the
11 measured spatial variability in ambient extinction with lesser contributions from variability in
12 relative humidity (10%) and aerosol composition (1.3%). On average, changes in aerosol
13 loading also caused 82% of the diurnal variability in ambient aerosol extinction. However on
14 days with relative humidity above 60%, variability in RH was found to cause up to 62% of the
15 spatial variability and 95% of the diurnal variability in ambient extinction.

16 This work shows that extinction is driven to first-order by aerosol mass loadings; however,
17 humidity-driven hydration effects play an important secondary role. This motivates combined
18 satellite/modelling assimilation products that are able to capture these components of the
19 AOD-PM_{2.5} link. Conversely, aerosol hygroscopicity and SSA play a minor role in driving
20 variations both spatially and throughout the day in aerosol extinction and therefore AOD.
21 However, changes in aerosol hygroscopicity from day-to-day were large and could cause a
22 bias of up to 27% if not accounted for. Thus it appears that a single daily measurement of
23 aerosol hygroscopicity can be used for AOD-to-PM_{2.5} conversions over the study region (on
24 the order of 1400 km²). This is complimentary to the results of Chu et al. (2015) that
25 determined the aerosol vertical distribution from “a single lidar is feasible to cover the range
26 of 100 km” in the same region.

27

28 **1 Introduction**

29 Aerosols are detrimental to human health and are regulated as a criteria pollutant by the
30 United States Environmental Protection Agency (EPA, 2014) and international agencies
31 (Vahlsing and Smith, 2012) with compliance based on measurements at ground sites.
32 However, satellites allow for the measurement of atmospheric conditions with a larger spatial

1 coverage than possible with a ground-based network of instruments and thus have the
2 potential to be useful tools in diagnosing ground-level air quality, particularly of aerosols (Al-
3 Saadi et al., 2005). Additionally, satellites have the advantage of detecting regional air
4 quality events in areas without historical air quality problems which thus have no or limited
5 ground-based sensor stations.

6 In order to relate satellite aerosol measurements to surface air quality, the connection between
7 aerosol optical depth (AOD) measured by satellites to ground-level fine-mode aerosol mass
8 ($PM_{2.5}$) must be known. The relationship between AOD and $PM_{2.5}$ has been widely studied
9 (Hoff and Christopher, 2009 and the references therein; Crumeyrolle et al., 2014 for the
10 current region) and ground-level $PM_{2.5}$ has been estimated based on AOD measurements both
11 empirically (Liu et al., 2005) and through the use of global models. Van Donkelaar et al.
12 (2006) found that the relative vertical extinction profile is the most important factor in the
13 AOD-to- $PM_{2.5}$ relationship. Thus this relationship is weakest in regions where the vertical
14 distribution cannot be reasonably modelled and is best in regions with fairly uniform aerosol
15 type and vertical distribution (well-mixed boundary layer with minimal free tropospheric
16 aerosol) such as the Northeast U.S. (Engel-Cox et al., 2004). Based on lidar measurements in
17 the Baltimore, MD – Washington, D.C. region, Chu et al. (2015) suggested that a single lidar
18 could provide adequate information on the vertical distribution to allow for retrievals of $PM_{2.5}$
19 from AOD measurements made within 100 km of the lidar. However, the AOD- $PM_{2.5}$
20 relationship is not only dependent on the aerosol vertical distribution but also variability in
21 aerosol composition and relative humidity (RH), both of which can be large in urban areas
22 due to the densely located nature of local and regional sources. This work is an analysis of
23 spatial and temporal variability in aerosol loading, composition and RH in the Baltimore, MD
24 – Washington, D.C. region and their effect on variability in aerosol extinction.

25 DISCOVER-AQ (Deriving Information on Surface conditions from Column and Vertically
26 Resolved Observations Relevant to Air Quality) was a multi-city NASA project designed to
27 better elucidate the connection between satellite measurements and air quality by studying the
28 variability in gas-phase and particulate pollutants in urban environments. The first campaign
29 was performed in the Baltimore-Washington region in July 2011 and combined remote
30 sensing instruments on the NASA Langley UC-12 flying at 9 km, ground-based observations
31 at multiple sites throughout the region, and in situ airborne measurements from the NASA
32 Wallops P-3B for the detailed analysis of atmospheric composition in the Baltimore-

1 Washington urban airshed. The P-3B flight plans (Fig. 1) were consistent among the 14
2 flights over 29 days to provide meaningful statistics (Table 1).

3 DISCOVER-AQ provides a valuable dataset to determine the variability in aerosol extinction
4 throughout the region. However, it is important to note that changes in aerosol extinction are
5 not necessarily solely due to an increase or decrease in aerosol loadings but can also be
6 indicative of variability in relative humidity and aerosol composition. Thus these data will be
7 used to examine:

8 1) The influence that aerosol loading, composition and relative humidity have on variability in
9 aerosol extinction in the Baltimore-Washington region; and

10 2) The spatial and temporal resolution requirements of these parameters necessary to
11 reproduce the variability in aerosol extinction.

12 These questions are relevant to scientists and policy makers seeking to assess the ability of
13 satellite AOD retrievals to diagnose ground-level air quality.

14

15 2 Experimental Design

16 The NASA P-3B was equipped with a variety of in situ aerosol and gas-phase measurements.

17 The current analysis uses a subset of these measurements including aerosol scattering,
18 absorption, size-distribution and composition. [Air was sampled with an isokinetic inlet which](#)
19 [efficiently collects and transmits particles with a diameter smaller than 4 \$\mu\text{m}\$ \(McNaughton et](#)
20 [al., 2007\).](#) Scattering coefficients at 450, 550 and 700 nm were measured with an integrating
21 nephelometer (TSI, Inc. model 3563) and corrected for truncation errors according to
22 Anderson and Ogren (1998), while absorption coefficients at 470, 532 and 660 nm were
23 measured with a Particle Soot Absorption Photometer (PSAP, Radiance Research) and
24 corrected for filter scattering according to Virkkula (2010). In order to calculate extinction,
25 the measured Angstrom exponent was used to adjust the scattering at 550 nm to 532 nm
26 (Ziemba et al., 2013).

27 During sampling, the RH of the air is modified due to the temperature gradient between the
28 outside and inside of the plane. This causes a change in the scattering coefficient due to the
29 generally hygroscopic nature of aerosol. To provide a stable scattering signal, the sample is
30 initially dried to approximately 20% RH utilizing a nafion drier and then sampled with
31 tandem nephelometers (with and without humidification) to find the dry ($\sigma_{\text{scat,dry}}$ at a RH_{dry} of

Deleted: Air was sampled with an isokinetic inlet which efficiently collects and transmits particles with a diameter smaller than 4 μm (McNaughton et al., 2007).

1 approximately 20%) and humidified scattering coefficients ($\sigma_{\text{scat,wet}}$ at a RH_{wet} of
2 approximately 80%). These scattering measurements are related via a single-parameter
3 monotonic growth curve (Gasso et al., 2000)

$$4 \quad \sigma_{\text{scat,wet}} = \sigma_{\text{scat,dry}} \cdot \left[\frac{100 - \text{RH}_{\text{wet}}}{100 - \text{RH}_{\text{dry}}} \right]^{-\gamma} \quad (1)$$

5 where γ is an experimentally determined variable of the hygroscopicity with water-uptake
6 increasing with increasing γ . $\sigma_{\text{scat,dry}}$ was corrected to 20% RH based on Eq. (1) to account for
7 any variability in RH_{dry} . Once γ is determined, the scattering at ambient RH ($\sigma_{\text{scat,amb}}$, RH_{amb})
8 is found from

$$9 \quad \sigma_{\text{scat,amb}} = \sigma_{\text{scat,dry}} \cdot \left[\frac{100 - \text{RH}_{\text{amb}}}{80} \right]^{-\gamma} \quad (2)$$

10 Ambient RH was calculated based on measurements of water vapor concentration by an open-
11 path diode laser hygrometer (Diskin et al., 2002), static temperature and pressure. Aerosol
12 extinction at ambient RH ($\sigma_{\text{ext,amb}}$) can then be found by summing $\sigma_{\text{scat,amb}}$ and absorption
13 (σ_{abs})

$$14 \quad \sigma_{\text{ext,amb}} = \sigma_{\text{scat,dry}} \cdot \left[\frac{100 - \text{RH}_{\text{amb}}}{80} \right]^{-\gamma} + \sigma_{\text{abs}} \quad (3)$$

15 The dependence of aerosol absorption on RH is highly uncertain (Redemann et al., 2001;
16 Mikhailov et al., 2006; Brem et al., 2012) and is therefore not incorporated but likely
17 manifests as only a small uncertainty in total extinction due to the fact that absorption was
18 only a minor component of extinction (4% on average).

19 Ziemba et al. (2013) showed a good correlation (R^2 of 0.88 [based on comparison of 668 data](#)
20 [points](#)) between extinction measurements from the P-3B and coincident measurements
21 performed by a high spectral resolution lidar (HSRL) on the UC-12. Recent work (Brock et
22 al., [2015a](#); Wagner et al., 2015) have suggested an additional model for aerosol
23 hygroscopicity known as the kappa (κ) parameterization. However, these two models (based
24 on γ and κ) are fairly consistent (scattering within 5%) at RHs below 85%, a range which
25 comprised 96% of the data measured by the P-3B. In addition, the good agreement between
26 HSRL and in situ data (utilizing the γ correction scheme) suggest this is a valid model for the
27 aerosol measured in Baltimore during DISCOVER-AQ (Ziemba et al., 2013).

Deleted: in preparation

1 Single scattering albedo (SSA) describes the relationship between aerosol scattering and
2 extinction:

$$3 \quad SSA = \left(\frac{\sigma_{scat,dry}}{\sigma_{ext,dry}} \right) = \left(\frac{\sigma_{scat,dry}}{\sigma_{scat,dry} + \sigma_{abs}} \right). \quad (4)$$

4 SSA can vary with RH (as scattering increases) but is here defined as the SSA under dry
5 conditions (20% RH). Thus Eq. (3) can be rewritten as

$$6 \quad \sigma_{ext,amb} = \sigma_{ext,dry} \cdot \left[1 + SSA \cdot \left(\left[\frac{100 - RH_{amb}}{80} \right]^{-\gamma} - 1 \right) \right]. \quad (5)$$

7 Black carbon (BC) mass was measured with a Single Particle Soot Photometer (SP2, Droplet
8 Measurement Technologies) while a pair of Particle-Into-Liquid Samplers (PILS, Brechtel
9 Manufacturing, Inc.; Weber et al., 2001) were used to measure water-soluble organic and
10 inorganic species. The PILS captures particles in the sampled air flow into a liquid flow of
11 deionized water. Denuders prior to the PILS removed gas-phase organic compounds (parallel
12 plate carbon filter denuders, Sunset Laboratory, Inc.) and inorganic acids and bases (annular
13 denuders coated with sodium carbonate and phosphoric acid, URG Corporation). Laboratory
14 testing prior to the campaign showed the use of denuders resulted in a size cut of
15 approximately 2 microns for the PILS systems.

Deleted: ;

Deleted: Th

Deleted: likely

Deleted:

16 The first PILS was coupled to a total organic carbon (TOC) analyzer (Sievers Model 800) to
17 give the mass of water-soluble organic carbon (WSOC) at a 10-second time resolution. The
18 TOC analyzer reports the organic carbon mass in $\mu\text{gC m}^{-3}$ and not the total organic mass
19 (which includes mass due to bonded hydrogen and oxygen atoms). Thus, to determine total
20 water-soluble organic matter (WSOM), a multiplier ranging from 1.6 for urban to 2.1 for non-
21 urban aerosols must be applied (Turpin and Lim, 2001). For the present work, a value of 1.8
22 is used based on Hand and Malm (2007). However, it should be noted that this does not
23 include mass from any water-insoluble organic compounds.

24 The liquid flow from the second PILS was collected in vials at a resolution of 3.25 or 5
25 minutes for off-line ion chromatographic (IC) analysis of chloride, nitrate, nitrite, sulfate,
26 sodium, ammonium, potassium, magnesium, and calcium mass concentrations. The IC
27 (Dionex ICS-3000 with an auto-sampler) utilized a CS12A column for cation analysis and an
28 AS11 column for anion analysis with run times of 15 and 20 minutes, respectively. Standards
29 were run periodically for calibration and to ensure system stability. Dilution was measured in

1 the PILS through the addition of lithium bromide to its water supply. Complete inorganic
2 composition data are not available from the first three flights due to contamination from the
3 sample vials; alternate vials were used for the remainder of the campaign. Aerosol size
4 distributions were measured with an Ultra-High Sensitivity Aerosol Spectrometer (UHSAS,
5 Droplet Measurement Technologies) calibrated with ammonium sulfate. All data are publicly
6 available from the NASA Langley Atmospheric Science Data Center (ASDC, 2015).

Deleted: Lithium bromide was added to the water supply to measure the dilution factor in the PILS.

7 As the PILS is unable to measure insoluble aerosol, the measured aerosol mass is a lower
8 limit for the actual mass. The PILS mass can be compared to the volume measured by the
9 UHSAS utilizing a density determined based on the measured mass of organics (1.2 g cm^{-3} ,
10 Turpin and Lim, 2001) and ammonium sulfate (1.77 g cm^{-3}). Based on this analysis, the PILS
11 measured approximately 82% of the aerosol mass with the other 18% assumed to be insoluble
12 organic compounds. Higher insoluble organic masses are estimated for higher loadings days
13 with insoluble loadings near zero for low loading days. However, this analysis has a large
14 uncertainty due to a difference in size range measured by the two instruments and
15 volatilization of aerosol at the PILS tip. Measurements by Sorooshian et al. (2006) show that
16 slightly more than 10% of the ammonium is lost in the PILS with a tip temperature of
17 approximately 100°C. Good closure (slope of 0.98) between cations and anions (equivalence)
18 suggests that any loss mechanisms are equivalent for all species. Thus, while this analysis
19 gives an approximation of possible insoluble mass, this estimation is not included in future
20 analysis due to the high uncertainty.

Deleted: Research Center

Deleted: W

Deleted: the uncertainty is high and therefore

Deleted: insoluble mass

22 3 Results – Mission Overview

23 Each DISCOVER-AQ-Maryland flight can be broken into two to three repetitive circuits
24 which encompassed spirals from 0.3 to 4.5 km centered over six primary ground sites
25 (labelled as Sites 1-6 in Fig. 1). If time permitted, additional spirals were performed at select
26 sites at the end of the flight resulting in 2 to 4 spirals over each site per flight. A time series
27 of aerosol extinction during Flight 9 highlights an altitude dependence of aerosol scattering,
28 with values oscillating between near-zero in the free troposphere and greater than 200 Mm^{-1}
29 in the mixing layer (Fig. 2).

30 The repetitive flight plan allows for the analysis of differences in aerosol properties and their
31 vertical distributions at each site as source profiles and boundary layer dynamics changed
32 during the day, as seen for Flight 9 in Fig. 3. During the first circuit (11:00-13:30 local time),

1 a mixed layer up to 1.5 km is seen capped by a residual layer between 1.5 and 2.5 km.
2 Surface heating causes the two layers to merge by the time the second circuit was performed
3 (13:30-15:30) with fairly constant extinction to 1.5 km and a gradual decrease to near-zero
4 extinction by 2.5 km. Circuit 3 (15:30-17:30) had constant extinction below 1.5 km but little
5 indication of a residual layer. In addition, the profiles among the sites become more
6 homogeneous as the day progresses (Fig. 3). In general, the mixing layer was consistently
7 greater than 1 km throughout the flights; therefore, data below 1 km is used as a measure of
8 mixing layer aerosol properties.

9 Aerosol mass loadings varied by a factor of six (Fig. 4) between the flights with average
10 aerosol mass in the lowest 1 km ranging from 3.8 to 26 $\mu\text{g m}^{-3}$. Aerosol optical
11 measurements varied by an even greater amount with ambient aerosol extinction in the lowest
12 1 km ranging from 20 to 290 Mm^{-1} and AODs (calculated from the integration of the
13 extinction profile) ranging from 0.05 to 0.57. In situ AOD measurements showed good
14 agreement (within 0.04) with ground-based radiometer measurements by the Aerosol Robotic
15 Network (AERONET, Holben et al., 2014) in the region (Ziemba et al., in preparation). The
16 fact that the highest extinction below 1 km (Flight 9) and AODs (Flight 14) were not
17 measured during the same flights highlights the potential disconnect between AOD and
18 surface layer aerosol loading. Flight 14 had a deeper aerosol layer and more aerosol in an
19 elevated layer than Flight 9 (Fig. 5); thus Flight 14 had a higher AOD despite having less
20 near-surface extinction than Flight 9. Other surface-independent factors influencing AOD
21 may include aerosol cloud-processing. Indeed, Eck et al. (2014) observed large increases in
22 AOD (average of 25%) in the vicinity of non-precipitating cumulus clouds. Consistent with
23 these findings, in situ measurements showed increases in aerosol scattering, volume and mass
24 in spirals measured before and after cloud formation. These included a doubling of water-
25 soluble organics and 50% increase in sulfate.

26 In general, the fraction of aerosol measured was primarily a mixture of WSOM (campaign
27 average of 57% by mass, Fig. 4), sulfate (23%) and ammonium (10%) with minor
28 contributions from nitrate (2.1%), BC (2.2%), chloride (2.0%) and sodium (1.3%). The molar
29 ratio of ammonium to sulfate was 1.92 showing that sulfate is almost completely neutralized
30 as ammonium sulfate, $(\text{NH}_4)_2\text{SO}_4$, with minimal bisulfate, $(\text{NH}_4)\text{HSO}_4$. Further, this ratio is
31 higher (above 2) if PILS volatilization of ammonium (12% loss of mass, Sorooshian et al.,
32 2006) and sulfate (1% loss) is considered. Composition varied between flights with polluted

Deleted: to ammonium

Deleted: Additionally

1 days (as noted in Fig. 4) exhibiting a higher fraction of ammonium and sulfate. Back-
2 trajectory analysis with the Hybrid Single Particle Lagrangian Integrated Trajectory Model
3 (HYSPLIT; Draxler and Hess, 1998; Draxler and Rolph, 2015) suggested these high aerosol
4 loading days were related to long-range transport from the Ohio River Valley (Fig. 6) which
5 has enhanced sulfur dioxide emissions due to a high density of coal-fired power plants in the
6 region (Hand et al., 2012). These days were generally associated with low pressure systems
7 to the northwest of the study region. Conversely, low loading days tended to have northerly
8 flow due to high pressure systems to the west.

9 The flights with transport from the west and higher aerosol loadings (starred in Fig. 4) were
10 found to have relatively more sulfate (28% of mass compared to 15% for clean days) and
11 ammonium (polluted, 11%; clean, 7.5%) and less organics (polluted, 52%; clean, 65%). Less
12 polluted days had higher percentages of nitrate (polluted, 1.1%; clean, 3.9%) and BC
13 (polluted, 2.0%; clean, 2.7%). The higher BC mass percentage also leads to higher absorption
14 relative to scattering and therefore lower SSA on these less polluted days (polluted, 0.98;
15 clean, 0.93; Fig. 7). However, on an absolute basis the polluted days had higher BC and
16 absorption than on the clean days. Average BC concentrations for the entire month were 240
17 ng m^{-3} in the lowest 1 km decreasing to 35 ng m^{-3} in the free troposphere (above 3 km).

18 The polluted flight days also had higher γ values (Fig. 7, Equation 5). This water-uptake is
19 largely dependent on aerosol composition with soluble organics having lower hygroscopicity
20 than inorganic compounds. This can be seen as an inverse relationship with $\gamma = 0.60 - 0.0042$
21 \times organic mass fraction (Fig. 8). These values are intermediate between measurements made
22 in other urban areas (Asia and U.S., Quinn et al., 2005; Texas, Massoli et al., 2009) and in the
23 remote atmosphere (the Indian Ocean, Quinn et al., 2005). Differences are likely due to
24 differences in the measurement of organics; the current study uses PILS to measure only
25 water-soluble organics while the other studies use aerosol mass spectrometry or thermo-
26 optical methods which are sensitive to all organic species. In addition to an elevated γ , high
27 loading days were typically more humid ($64 \pm 7\%$ compared to $49 \pm 7\%$). These higher
28 humidities and γ -values resulted in a higher water content of the aerosols as evident from
29 ambient extinctions that were 25% higher than dry values on high loading days compared to
30 the 12% observed on low loading days. The highest daily-averaged water content of aerosol
31 extinction was 40% measured during Flight 8.

Deleted: ammonium

Deleted: 3

Deleted: 20

Deleted: ammonium

Deleted: 4

Deleted: 5

Deleted: ammonium sulfate and ammonium nitrate

1 Aerosol mass is the primary measurement of aerosol loading and the basis by which ground
2 air quality is regulated. Boundary layer dry extinction, ambient extinction and AOD are
3 additional measures of aerosol loading in combination but incorporate an increasing amount
4 of confounding factors. For instance, dry extinction is dependent on the aerosol mass loading
5 in addition to aerosol size and composition. Ambient extinction is dependent on these same
6 factors plus the aerosol hygroscopicity and RH. Finally, AOD is also dependent on the
7 vertical distribution of aerosols and RH. ~~Aerosol mass loading, dry extinction (not shown),~~
8 ~~ambient extinction and AOD follow similar trends (Fig. 4) suggesting that aerosol mass~~
9 ~~loadings are the primary factor controlling day-to-day variability in aerosol optical properties.~~
10 However, aerosol mass measurements via PILS do not account for insoluble aerosol. Dry
11 mass extinction efficiencies calculated from extinction and mass measurements were variable
12 ranging between 3.2 and 8.3 m² g⁻¹. The highest mass extinction efficiencies (measured on
13 high loading days) likely are indicative of the presence of insoluble organic material.
14 Therefore, because of the variable quantity of insoluble mass and the low time resolution of
15 the PILS measurements, future analysis will use the dry extinction as a proxy for aerosol
16 loadings.

17

18 **4 Results – Regional Variability**

19 Aerosol extinction varied not only on a temporal basis (Fig. 4) but also spatially. Because
20 there is such a large difference in aerosol loadings, optical properties (related to composition)
21 and RH between flights, using campaign averages would distort the spatial trends. Therefore,
22 each circuit consisting of spirals over six ground sites is treated as a separate ‘snapshot’ of the
23 region and the properties measured over each site are normalized to the circuit average to
24 study the spatial variability. Data below 1 km pressure altitude were used for 34 circuits for
25 which spirals were performed over all six sites (absorption measurements were not available
26 for one additional circuit and therefore it was not included in this analysis).

27 In order to get a general overview of aerosol variability in the regional, the average
28 normalized dry and ambient extinctions along with RH for all of the circuits are shown in Fig.
29 9. The data is first normalized to the average for the circuit and then the normalized values
30 are averaged. The highest dry aerosol extinction was nearest downtown Baltimore with Site 5
31 extinction 5.6% larger than the average. However, the average ambient extinction measured
32 was highest at the north end of the region where Site 3 is 5.5% larger. This is consistent with

Deleted: To a first approximation (Fig. 4), a

Deleted: how

1 the observed latitudinal gradient in RH. This shows that meteorological conditions (RH) can
 2 alter spatial trends in ambient extinction. Theoretically, it is possible for the entire region to
 3 have the same aerosol loading but differing extinction due to variability in composition and
 4 RH. Conversely, it is possible that the entire region could have a gradient in aerosol loading
 5 yet the composition and RH vary in such a way that extinction is constant throughout the
 6 region.

7 However, in order to study aerosol variability it is important to analyze each circuit
 8 individually (and not as a campaign average as done in Fig. 9). Eq. (5) shows the dependence
 9 of aerosol ambient extinction on aerosol loading ($\sigma_{ext,dry}$), composition (SSA and γ) and RH,
 10 and can be used as a simple model to determine the factors controlling aerosol ambient
 11 extinction. From this, an assessment of the accuracy needed for each of these parameters to
 12 relate aerosol extinction (which can be derived from satellite measurements) to aerosol
 13 loading can be performed. In order to determine the relative importance of aerosol loading,
 14 composition and RH on extinction, the partial derivatives of Eq. (5) can be determined:

$$15 \quad \frac{\partial \sigma_{ext,amb}}{\partial \sigma_{ext,dry}} = 1 + SSA \cdot \left(\left[\frac{100 - RH_{amb}}{80} \right]^{-\gamma} - 1 \right), \quad (6)$$

$$16 \quad \frac{\partial \sigma_{ext,amb}}{\partial SSA} = \sigma_{ext,dry} \cdot \left(\left[\frac{100 - RH_{amb}}{80} \right]^{-\gamma} - 1 \right), \quad (7)$$

$$17 \quad \frac{\partial \sigma_{ext,amb}}{\partial RH} = \frac{\sigma_{ext,dry} \cdot SSA \cdot \gamma}{80} \left[\frac{100 - RH_{amb}}{80} \right]^{-\gamma-1}, \quad (8)$$

$$18 \quad \frac{\partial \sigma_{ext,amb}}{\partial \gamma} = -\sigma_{ext,dry} \cdot SSA \cdot \left[\frac{100 - RH_{amb}}{80} \right]^{-\gamma} \cdot \ln \left(\frac{100 - RH_{amb}}{80} \right). \quad (9)$$

19 As expected, ambient extinction is linear with dry extinction (the partial derivative does not
 20 contain $\sigma_{ext,dry}$). The positive linear dependence on SSA shows that if all other variables are
 21 held constant, as SSA increases scattering becomes a larger fraction of extinction and at any
 22 RH above 20% will cause an increase in extinction due to water uptake. The dependence on
 23 RH and γ are both non-linear and thus their effects are most important when the RH is high or
 24 the aerosol is very hygroscopic.

25 Equations 6 through 9 can be combined to give the total differential for $\sigma_{ext,amb}$

$$1 \quad d\sigma_{ext,amb} = \frac{\partial\sigma_{ext,amb}}{\partial\sigma_{ext,dry}} \cdot d\sigma_{ext,dry} + \frac{\partial\sigma_{ext,amb}}{\partial SSA} \cdot dSSA + \frac{\partial\sigma_{ext,amb}}{\partial RH} \cdot dRH + \frac{\partial\sigma_{ext,amb}}{\partial\gamma} \cdot d\gamma. \quad (10)$$

2 Assuming that the four variables are independent

$$3 \quad s(\sigma_{ext,amb}) = \left[\left(\frac{\partial\sigma_{ext,amb}}{\partial\sigma_{ext,dry}} \cdot s(\sigma_{ext,dry}) \right)^2 + \left(\frac{\partial\sigma_{ext,amb}}{\partial SSA} \cdot s(SSA) \right)^2 + \left(\frac{\partial\sigma_{ext,amb}}{\partial RH} \cdot s(RH) \right)^2 + \left(\frac{\partial\sigma_{ext,amb}}{\partial\gamma} \cdot s(\gamma) \right)^2 \right]^{1/2} \quad (11)$$

4 where $s(x)$ is the standard deviation in x which is used as a measure of the variability in
 5 measurements made at the six sites during one circuit. Each term signifies the explained
 6 variance due to each of the four properties. Thus the relative contribution (RC) of dry aerosol
 7 scattering to the variability in ambient extinction in the region can then be found by:

$$8 \quad RC(\sigma_{ext,dry}) = \frac{\left(\frac{\partial\sigma_{ext,amb}}{\partial\sigma_{ext,dry}} \cdot s(\sigma_{ext,dry}) \right)^2}{s(\sigma_{ext,amb})^2}. \quad (12)$$

9 Using this method, the RC for each of the four variables can be determined for each circuit.

10 In order to determine the relative contribution of each factor on the variability in ambient
 11 aerosol extinction, each circuit was analyzed separately. Shown in Fig. 10 are two extreme
 12 cases. During Flight 1, ambient relative humidity was low ($37 \pm 4\%$) resulting in little water
 13 uptake (the shaded portion on the upper panel). Thus variability in dry extinction (aerosol
 14 loading) is the major contributor ($RC(\sigma_{ext,dry}) = 99\%$) to variability in ambient extinction. The
 15 second case during Flight 14 shows a period of high RH ($64 \pm 8\%$). Water uptake was
 16 substantial and greatest at Site 3 where the RH is the highest. In this case, the variability in
 17 aerosol extinction is not only dependent on variability in dry extinction (41%) but also
 18 relative humidity (57%).

19 On average, aerosol loading (dry extinction) accounted for 88% of the spatial variability in
 20 extinction, with 27 of the 34 complete circuits having $RC(\sigma_{ext,dry})$ above 80% (Fig. 11).
 21 Variability in RH only accounted for 10% of the ambient extinction variability on average
 22 with only 5 circuits having $RC(RH)$ greater than 20%. Four of these cases where RH had a
 23 large effect on ambient extinction variability corresponded to days with high RH (above
 24 60%). This is due to the non-linearity of extinction with respect to RH (Eq. (8)). Thus at low

1 relative humidities, changes in RH minimally impact ambient extinction. Conversely, when
2 RHs are high, small changes can produce large variations in ambient extinction. Changes in γ
3 and SSA were smaller contributors to ambient extinction variability (1.3% and less than 0.1%
4 on average, respectively).

5

6 **5 Results – Diurnal Variability**

7 A similar analysis can be performed to examine the diurnal variability of aerosol extinction.
8 For this analysis, each variable was averaged for each of the six sites during each flight. This
9 produced data at each spiral site approximately every 2 hours during each flight period (3 to 4
10 values per site per day); the comparison between these values were then used to determine the
11 diurnal variability in each parameter over the course of each flight. Sites with only two
12 spirals during a flight were not included in this analysis. Figure 12 shows data at Site 4 from
13 the same flights used for the regional variability analysis. For Flight 1, little water uptake
14 occurred during the flight period so more than 99% of the diurnal change in ambient
15 extinction is due to changes in aerosol loading. In contrast, during Flight 14, extinction
16 variability is dependent on both changes in aerosol loading and RH (51 and 49%,
17 respectively). From the first to second circuit, ambient extinction dropped as a result of an
18 RH change from 70% to 59%. After 16:00 local time, the RH continued to drop but ambient
19 extinction increased due to an increase in dry aerosol extinction. Thus in this case,
20 knowledge of the aerosol loading and RH trends are needed to interpret the aerosol extinction
21 diurnal trends. On average, diurnal extinction variability was dominated by changing aerosol
22 loading (82%) with smaller contributions from changes in RH, γ and SSA (16%, 1.6% and
23 less than 0.1%, respectively). However, RC(RH) values greater than 90% were measured
24 during Flight 9 (highest orange markers on the right panel of Fig. 11), a day with high RH and
25 highly variable RH.

26 **6 Discussion**

27 The conversion of extinction at ambient RH to extinction at a reduced (“dry”) RH is
28 important in relating remote sensing measurements of ambient extinction to dry aerosol mass.
29 Though the analysis above shows that variability in γ and SSA are only minor contributors to
30 ambient extinction variability, converting between ambient and dry extinction requires
31 knowledge of both parameters, as evident by Eq. (3). However, both γ and SSA are not
32 routinely measured at air quality monitoring sites. So the question could be asked “At what

Deleted: the

Deleted: was as high as 95%

Deleted: (Fig. 11)

1 frequency (both spatially and temporally) do γ and SSA need to be known to determine the
2 proper RH conversion?" This can be examined by analyzing the DISCOVER-AQ-Maryland
3 data recorded below 1 km and determining how using more averaged data yields differing
4 ambient aerosol extinctions.

5 As a result of changes in composition seen in Fig. 4, γ varied between 0.14 (Flight 1) and 0.47
6 (Flight 8) with an average of 0.32 (Fig. 13). Comparing the ambient extinction calculated
7 during each spiral with the extinction calculated using the daily average γ resulted in a bias of
8 $\pm 1.6\%$ in ambient extinction with no clear trend with respect to aerosol extinction. Using the
9 monthly average for the entire region causes a bias of $\pm 6.8\%$ (Table 2) with deviations of up
10 to 27% at high aerosol extinction because γ tended to be higher on high aerosol loading days
11 (Fig. 8). We conclude that spatial γ differences in the Baltimore region are not large enough
12 to cause significant biases in deriving dry extinction from ambient values. However, day-to-
13 day variability in γ can cause large discrepancies. Thus it appears that a single daily
14 measurement of γ (or one based on compositional measurements, Fig. 8) is able to be used for
15 AOD-to-PM_{2.5} correlations over the study region (on the order of 1400 km²) within an
16 uncertainty of 2%.

17 A similar analysis can be performed to evaluate the importance of SSA in retrieving dry
18 extinction from ambient extinction (Fig. 14 and Table 2). SSA varied from 0.91 to 0.99
19 during the mission with higher SSA measured on high aerosol loading days due to the
20 increased loading of sulfate and other secondary aerosols which are typically more scattering
21 than primary aerosols. Comparing the ambient extinction calculated during each spiral with
22 the extinction calculated using the daily average SSA resulted in a bias of $\pm 0.2\%$ in ambient
23 extinction showing that regional variability in SSA was not high enough to make a significant
24 difference. Using the monthly average for the entire region produces biases of $\pm 0.5\%$ with
25 deviations of up to 1.0% at high aerosol extinction.

26 Doing the same analysis for dry aerosol extinction or RH show markedly different results
27 (Fig. 15 and 16, Table 2). The use of a daily average dry extinction causes a bias of $\pm 22\%$
28 showing that regional variation in aerosol loading must be accounted for. Utilizing a monthly
29 average extinction causes discrepancies of $\pm 111\%$ due to the large day-to-day variability in
30 aerosol loading. Biases based on limited knowledge of RH were smaller with $\pm 6.2\%$ for daily
31 and 11% for monthly RH. Thus, Table 2 gives a hierarchy of factors for variability in
32 extinction measurements: loading > RH > γ > SSA.

Deleted: ammonium

1 An analysis of the effects of aerosol and meteorological parameters on AOD in the
2 Southeastern U.S. based on 37 airborne profiles (Brock et al., [2015b](#)) show similar trends in
3 the significance of factors with aerosol mass the most important. Relative humidity had a
4 non-linear significance on AOD with the greatest significance for extremely humid conditions
5 (the 90th percentile RH profiles). Varying aerosol size parameters and the vertical
6 distribution of the aerosols resulted in moderate AOD changes, while AODs were largely
7 insensitive to refractive index in a fashion similar to the present findings of SSA as a minor
8 contributor to extinction variability.

Deleted: in preparation

Deleted: ;

9

10 7 Conclusions

11 Measurements made in the Baltimore-Washington D.C. region during DISCOVER-AQ in
12 July 2011 can be generalized as follows: on days influenced by transport from the Ohio River
13 Valley, aerosol loadings were higher (aerosol mass concentrations of $18.7 \pm 4.4 \mu\text{g m}^{-3}$ and
14 AODs of 0.43 ± 0.12) and the aerosol were more hygroscopic (γ of 0.36 ± 0.07) because of a
15 larger percentage of ammonium and sulfate (38% of water-soluble mass) in comparison to
16 days impacted by northerly transport (aerosol masses of $5.4 \pm 1.3 \mu\text{g m}^{-3}$, AODs of $0.08 \pm$
17 0.03 , γ of 0.26 ± 0.09 , 20% ammonium and sulfate). In both cases, the regional and diurnal
18 variability in aerosol extinction are controlled primarily by changes in aerosol loadings.
19 However, on days associated with westerly transport (which also were more humid)
20 variability in RH also contributed significantly to the regional (14%) and diurnal (22%)
21 variability in extinction. Thus changes in AOD cannot directly be seen as changes in $\text{PM}_{2.5}$
22 but must take into account spatial and temporal variability in RH.

Deleted: such

23 Variability in aerosol composition (as indicated by γ and SSA) was found to have a very small
24 contribution to variability in aerosol extinction both diurnally and regionally. However, day-
25 to-day changes in γ were large enough that utilization of a monthly average would result in a
26 bias of $\pm 6.8\%$ in aerosol extinction with biases up to 27% for high aerosol loading days.
27 Thus, daily measurement of γ (or a value derived from compositional measurements) at one
28 location is needed to provide information for the entire study region. This is similar to the
29 results of Chu et al. (2015) that the aerosol vertical distribution from “a single lidar is feasible
30 to cover the range of 100 km” in the same region. However, this may not apply for regions
31 outside of the U.S. Northeast which have lower AOD-to- $\text{PM}_{2.5}$ correlation because of more
32 variable aerosol composition and vertical distributions (Engel-Cox et al., 2004).

1

2 **Acknowledgements**

3 This research was funded by NASA's Earth Venture-1 Program through the Earth System
4 Science Pathfinder (ESSP) Program Office. We thank the DISCOVER-AQ Science Team
5 especially the pilots and flight crews of NASA's P-3B. Boundary layer heights based on
6 airborne measurements of the potential temperature profile were provided by Don Lenschow
7 of the University Corporation for Atmospheric Research (UCAR). Thanks also to Joshua
8 DiGangi and Michael Shook (both of NASA Langley) for valuable discussions during
9 manuscript preparation.

10

1 **References**

2 ASDC: NASA Airborne Science Data for Atmospheric Composition: DISCOVER-AQ,
3 <http://www-air.larc.nasa.gov/cgi-bin/ArcView/discover-aq.dc-2011>, doi:
4 10.5067/Aircraft/DISCOVER-AQ/Aerosol-TraceGas, 2015.

5 Al-Saadi, J., Szykman, J., Pierce, R. B., Kittaka, C., Neil, D., Chu, D. A., Remer, L., Gumley,
6 L., Prins, E., Weinstock, L., MacDonald, C., Wayland, R., Dimmick, F., and Fishman, J.:
7 Improving National Air Quality Forecasts with Satellite Aerosol Observations, *Bulletin of the*
8 *American Meteorological Society*, 86, 1249–1261, 2005.

9 Anderson, T. L., and Ogren, J.A.: Determining Aerosol Radiative Properties using the TSI
10 3563 Integrating Nephelometer, *Aerosol Science and Technology*, 29, 57-69, 1998.

11 Brem, B. T., Mena Gonzalez, F. C., Meyers, S. R., Bond, T. C., and Rood, M. J.: Laboratory-
12 Measured Optical Properties of Inorganic and Organic Aerosols at Relative Humidities up to
13 95%, *Aerosol Science and Technology*, 46, 178–190, 2012.

14 [Brock, C. A., Wagner, N. L., Anderson, B. E., Attwood, A. R., Beyersdorf, A., Campuzano-
15 Jost, P., Carlton, A. G., Day, D. A., Diskin, G. S., Gordon, T. D., Jimenez, J. L., Lack, D. A.,
16 Liao, J., Markovic, M. Z., Middlebrook, A. M., Ng, N. L., Perring, A. E., Richardson, M. S.,
17 Schwarz, J. P., Washenfelder, R. A., Welti, A., Xu, L., Ziemba, L. D., and Murphy, D. M.:
18 *Aerosol optical properties in the southeastern United States in summer – Part 1: Hygroscopic
19 growth*, *Atmospheric Chemistry and Physics Discussions*, 15, 25695-25738,
20 \[doi:10.5194/acpd-15-25695-2015\]\(https://doi.org/10.5194/acpd-15-25695-2015\), 2015a.](#)

21 [Brock, C. A., Wagner, N. L., Anderson, B. E., Beyersdorf, A., Campuzano-Jost, P., Day, D.
22 A., Diskin, G. S., Gordon, T. D., Jimenez, J. L., Lack, D. A., Liao, J., Markovic, M.,
23 Middlebrook, A. M., Perring, A. E., Richardson, M. S., Schwarz, J. P., Welti, A., Ziemba, L.
24 D., and Murphy, D. M.: *Aerosol optical properties in the southeastern United States in
25 summer – Part 2: Sensitivity of aerosol optical depth to relative humidity and aerosol
26 parameters*, *Atmospheric Chemistry and Physics Discussions*, 15, 31471-31499,
27 \[doi:10.5194/acpd-15-31471-2015\]\(https://doi.org/10.5194/acpd-15-31471-2015\), 2015b.](#)

28 [Chu, D. A., Ferrare, R., Szykman, J., Lewis, J., Scarino, A., Hains, J., Burton, S., Chen, G.,
29 Tsaif, T., Hostetler, C., Hair, J., Holben, B., and Crawford, J.: Regional characteristics of the
30 relationship between columnar AOD and surface PM_{2.5}: Application of lidar aerosol](#)

Deleted: ¶

1 extinction profiles over Baltimore–Washington Corridor during DISCOVER-AQ,
2 Atmospheric Environment, 101, 338–349, 2015.

3 Crumeyrolle, S., Chen, G., Ziemba, L., Beyersdorf, A., Thornhill, L., Winstead, E., Moore, R.
4 H., Shook, M. A., Hudgins, C., and Anderson, B. E.: Factors that influence surface PM_{2.5}
5 values inferred from satellite observations: Perspective gained for the US Baltimore–
6 Washington metropolitan area during DISCOVER-AQ, Atmospheric Chemistry and Physics,
7 14, 2139-2153, 2014.

8 Diskin, G. S., Podolske, J. R., Sachse, G. W., and Slate, T. A.: Open-path airborne tunable
9 diode laser hygrometer, Proceedings of SPIE, 4817, 2002.

10 Draxler, R. R., and Hess, G. D.: An overview of the HYSPLIT-4 modeling system of
11 trajectories, dispersion, and deposition, Australian Meteorological Magazine, 47, 295-308,
12 1998.

13 Draxler, R. R., and Rolph, G. D.: NOAA Air Resources Laboratory HYSPLIT (HYbrid
14 Single-Particle Lagrangian Integrated Trajectory), <http://ready.arl.noaa.gov/HYSPLIT.php>,
15 2015.

16 [Eck, T. F., Holben, B. N., Reid, J. S., Arola, A., Ferrare, R. A., Hostetler, C. A., Crumeyrolle,
17 S. N., Berkoff, T. A., Welton, E. J., Lolli, S., Lyapustin, A., Wang, Y., Schafer, J. S., Giles,
18 D. M., Anderson, B. E., Thornhill, K. L., Minnis, P., Pickering, K. E., Loughner, C. P.,
19 Smirnov, A., and Sinyuk, A.: Observations of rapid aerosol optical depth enhancements in the
20 vicinity of polluted cumulus clouds, Atmos. Chem. Phys., 14, 11633-11656, doi:10.5194/acp-
21 14-11633-2014, 2014.](#)

22 Engel-Cox, J. A., Holloman, C. H., Coutant, B. W., and Hoff, R. M.: Qualitative and
23 quantitative evaluation of MODIS satellite sensor data for regional and urban scale air quality,
24 Atmospheric Environment, 38, 2495–2509, 2004.

25 EPA, 2014: National Ambient Air Quality Standards, <http://www.epa.gov/air/criteria.html>,
26 2015.

27 Gasso, S., Hegg, D. A., Covert, D. S., Collins, D., Noone, K. J., Ostrom, E., Schmid, B.,
28 Russell, P. B., Livingston, J. M., Durkee, P. A., and Jonsson, H.: Influence of humidity on the
29 aerosol scattering coefficient and its effect on the upwelling radiance during ACE-2, Tellus B,
30 52, 546–567, 2000.

1 Hand, J. L., and Malm, W. C.: Review of aerosol mass scattering efficiencies from ground-
2 based measurements since 1990, *Journal of Geophysical Research* 112, D16203, 2007.

3 Hand, J. L., Schichtel, B. A., Malm, W. C., and Pitchford, M. L.: Particulate sulfate ion
4 concentration and SO₂ emission trends in the United States from the early 1990s through
5 2010, *Atmospheric Chemistry and Physics*, 12, 10353–10365, 2012.

6 Hoff, R. M., and Christopher, S. A.: Remote Sensing of Particulate Pollution from Space:
7 Have We Reached the Promised Land?, *Journal of the Air & Waste Management Association*,
8 59, 645-675, 2009.

9 [Holben, B. N., Eck, T. F., Slutsker, I., Tanre, D., Buis, J. P., Setzer, A., Vermote, E., Reagan,](#)
10 [J. A., Kaufman, Y., Nakajima, T., Lavenu, F., Jankowiak, I., and Smirnov, A.: AERONET-A](#)
11 [federated instrument network and data archive for aerosol characterization, *Remote Sensing*](#)
12 [of *Environment*, 66, 1–16, 1998.](#)

13 Liu, Y., Sarnat, J. A., Kilaru, V., Jacob, D. J., and Koutrakis, P.: Estimating Ground-Level
14 PM_{2.5} in the Eastern United States Using Satellite Remote Sensing, *Environmental Science &*
15 *Technology*, 39, 3269-3278, 2005.

16 Massoli, P., Bates, T. S., Quinn, P. K., Lack, D. A., Baynard, T., Lerner, B. M., Tucker, S. C.,
17 Brioude, J., Stohl, A., and Williams, E. J.: Aerosol optical and hygroscopic properties during
18 TexAQS-GoMACCS 2006 and their impact on aerosol direct radiative forcing, *Journal of*
19 *Geophysical Research*, 114, D00F07, 2009.

20 McNaughton, C. S., Clarke, A. D., Howell, S. G., Pinkerton, M., Anderson, B., Thornhill, L.,
21 Hudgins, C., Winstead, E., Dibb, J. E., Scheuer, E., and Maring, H.: Results from the DC-8
22 Inlet Characterization Experiment (DICE): Airborne Versus Surface Sampling of Mineral
23 Dust and Sea Salt Aerosols, *Aerosol Science and Technology*, 41, 136–159, 2007.

24 Mikhailov, E. F., Vlasenko, S. S., Podgorny, I. A., Ramanathan, V., and Corrigan, C. E.:
25 Optical properties of soot–water drop agglomerates: An experimental study, *Journal of*
26 *Geophysical Research*, 111, D07209, 2006.

27 Quinn, P. K., Bates, T. S., Baynard, T., Clarke, A. D., Onasch, T. B., Wang, W., Rood, M. J.,
28 Andrews, E., Allan, J., Carrico, C. M., Coffman, D., and Worsnop, D.: Impact of particulate
29 organic matter on the relative humidity dependence of light scattering: A simplified
30 parameterization, *Geophysical Research Letters*, 32, L22809, 2005.

1 Redemann, J., Russell, P. B., and Hamill, P.: Dependence of Aerosol Light Absorption and
2 Single-Scattering Albedo on Ambient Relative Humidity for Sulfate Aerosols with Black
3 Carbon Cores, *Journal of Geophysical Research*, 106, 27485–27495, 2001.

4 [Sorooshian, A., Brechtel, F. J., Ma, Y. L., Weber, R. J., Corless, A., Flagan, R. C., and](#)
5 [Seinfeld, J. H.: Modeling and characterization of a particle-into-liquid sampler \(PILS\),](#)
6 [Aerosol Science and Technology, 40, 396-409, 2006.](#)

7 Turpin, B. J., and Lim, H.-J.: Species Contributions to PM_{2.5} Mass Concentrations:
8 Revisiting Common Assumptions for Estimating Organic Mass, *Aerosol Science and*
9 *Technology*, 35, 602–610, 2001.

10 Vahlsing, C., and Smith, K. R.: Global review of national ambient air quality standards for
11 PM₁₀ and SO₂ (24 h), *Air Quality, Atmosphere & Health*, 5, 393-399, 2012.

12 van Donkelaar, A., Martin, R. V., and Rokjin, J. P.: Estimating ground-level PM_{2.5} using
13 aerosol optical depth determined from satellite remote sensing, *Journal of Geophysical*
14 *Research*, 111, D21201, 2006.

15 Virkkula, A.: Correction of the calibration of the 3-wavelength Particle Soot Absorption
16 Photometer (3λ PSAP), *Aerosol Science and Technology*, 44, 706-712, 2010.

17 Wagner, N. L., Brock, C. A., Angevine, W. M., Beyersdorf, A., Campuzano-Jost, P., Day, D.,
18 de Gouw, J. A., Diskin, G. S., Gordon, T. D., Graus, M. G., Holloway, J. S., Huey, G.,
19 Jimenez, J. L., Lack, D. A., Liao, J., Liu, X., Markovic, M. Z., Middlebrook, A. M.,
20 Mikoviny, T., Peischl, J., Perring, A. E., Richardson, M. S., Ryerson, T. B., Schwarz, J. P.,
21 Warneke, C., Welti, A., Wisthaler, A., Ziemba, L. D., and Murphy, D. M.: In situ vertical
22 profiles of aerosol extinction, mass, and composition over the southeast United States during
23 SENEX and SEAC4RS: observations of a modest aerosol enhancement aloft, *Atmospheric*
24 *Chemistry and Physics*, 15, 7085-7102, 2015.

25 Weber, R. J., Orsini, D., Daun, Y., Lee, Y.-N., Klotz, P. J., and Brechtel, F.: A Particle-into-
26 Liquid Collector for Rapid Measurement of Aerosol Bulk Chemical Composition, *Aerosol*
27 *Science and Technology*, 35, 718–727, 2001.

28 Ziemba, L. D., Thornhill, K. L., Ferrare, R., Barrick, J., Beyersdorf, A. J., Chen, G.,
29 Crumeyrolle, S. N., Hair, J., Hostetler, C., Hudgins, C., Obland, M., Rogers, R., Scarino, A.
30 J., Winstead, E. L., and Anderson, B. E.: Airborne observations of aerosol extinction by in

1 situ and remote-sensing techniques: Evaluation of particle hygroscopicity, *Geophysical*
2 *Research Letters*, 40, 417-422, 2013.
3

1 Table 1. DISCOVER-AQ flight dates [including complete circuits over all six sites flown.](#)

Flight	Date (2011)	Circuits Flown
1	July 1	3
2	July 2	3
3	July 5	3
4	July 10	3
5	July 11	2
6	July 14	3
7	July 16	2
8	July 20	3
9	July 21	3
10	July 22	3
11	July 26	3
12	July 27	3
13	July 28	3
14	July 29	3

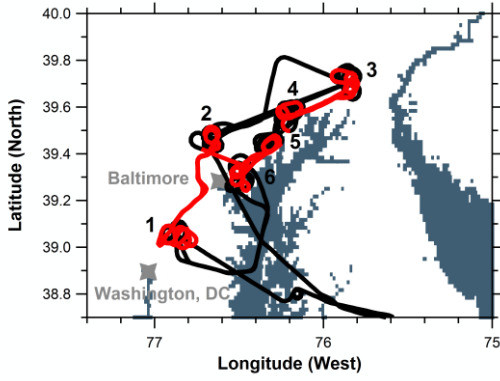
2

3

1 Table 2. Percent bias in ambient extinction based on daily and monthly averaging of
2 contribution variables.

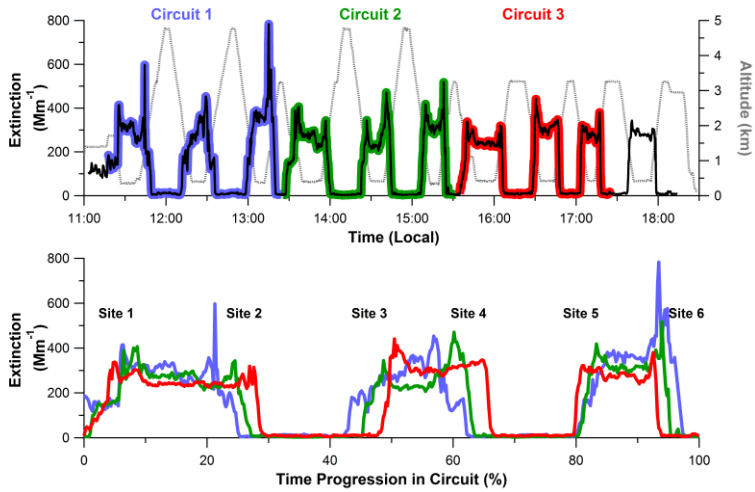
Variable	Percent Bias Based on Averaging	
	Daily	Monthly
Dry Extinction	22	111
RH	6.2	10.7
γ	1.6	6.8
SSA	0.21	0.49

3



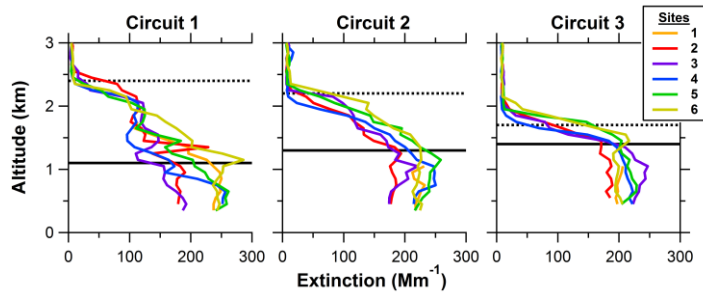
1
2
3
4
5
6
7
8

Figure 1. Flight path for Flight 1. Portions below 1 km are shown in red and those above in black. Flights originated at NASA Wallops Flight Facility (southeast of the area shown) to ground Sites 1 through 6 in order with a spiral performed at each site. The circuit was typically flown 3 times per flight before returning to Wallops. Water is denoted as blue with the Chesapeake Bay at the center and the Delaware Bay on the right edge.



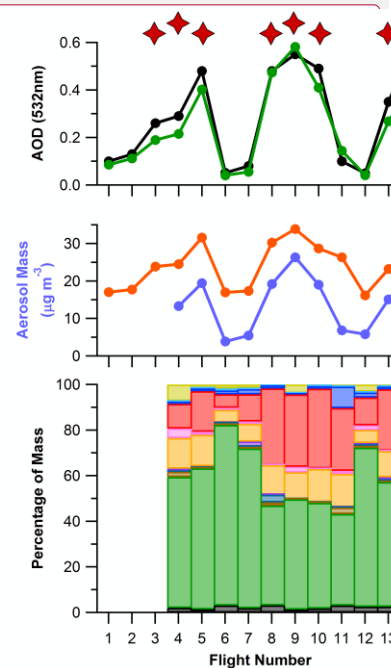
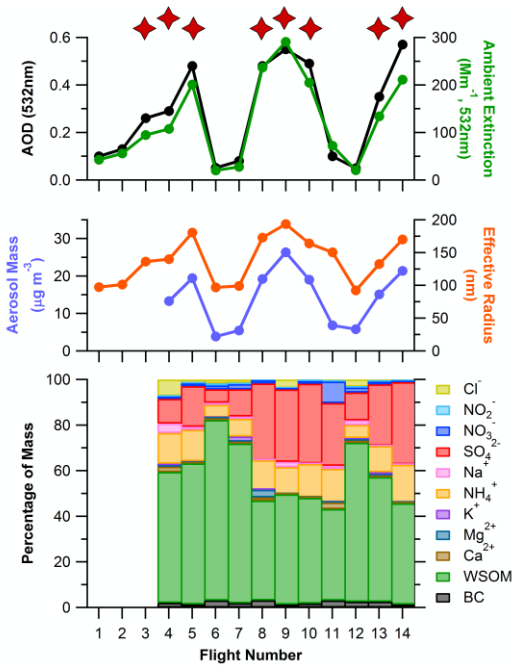
1
2
3
4
5
6
7

Figure 2. Time series of extinction (at ambient RH and 532 nm) and altitude (gray dashed line) for Flight 9 (upper panel). Extinction measurements during each circuit are highlighted by differing background color. Each circuit is then plotted in the bottom panel to show the changes in aerosol between the circuits. Profile locations correspond to those shown in Fig. 1.



1
2
3
4
5
6
7

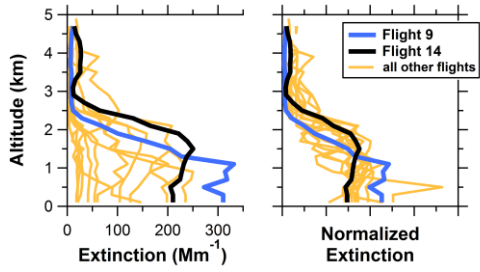
Figure 3. Vertical profiles of aerosol extinction (at ambient RH and 532 nm) for Flight 9 segregated by circuit and profile site. Horizontal lines represent the boundary layer (solid line) and buffer layer (dashed line) heights during each circuit at Site 2 based on airborne measurements of the potential temperature profile.



Deleted:

1
2
3
4
5
6
7

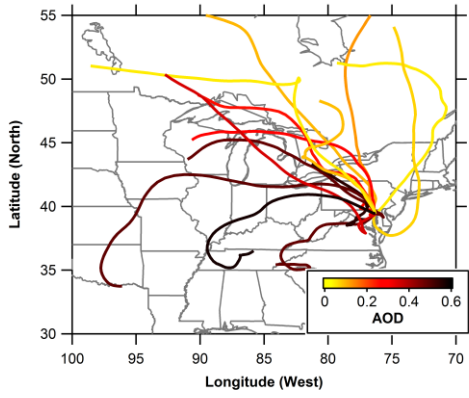
Figure 4. Average AOD (at ambient RH) along with boundary layer (below 1 km) extinction, aerosol mass, effective radius and composition for each of the fourteen flights. Aerosol mass and composition data are not available for the first three flights. Flights with predominantly westerly transport from the Ohio River Valley are indicated by stars at the top of the plots.



1
2
3
4
5
6
7
8

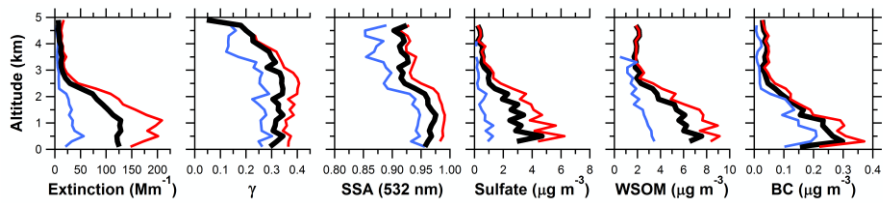
Figure 5. Average vertical profiles of aerosol extinction (at ambient RH and 532 nm) for all flights with Flights 9 and 14 highlighted (left panel). These profiles can then be normalized to the total aerosol loading (AOD) to get the normalized vertical profile (right panel, arbitrary units).

Deleted: left



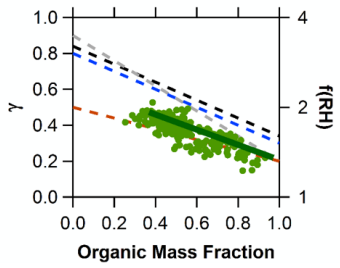
1
2
3
4
5
6

Figure 6. 72-hour back-trajectories based on HYSPLIT for the first circuit of each flight at Site 5 at an altitude of 1 km colored by the average AOD measured during that flight.



1
 2 Figure 7. Average profiles for extinction (at ambient RH and 532 nm), γ , SSA and
 3 composition for all flights (black line), days with predominantly westerly transport from the
 4 Ohio River Valley (red line), and days with northerly transport (blue line).

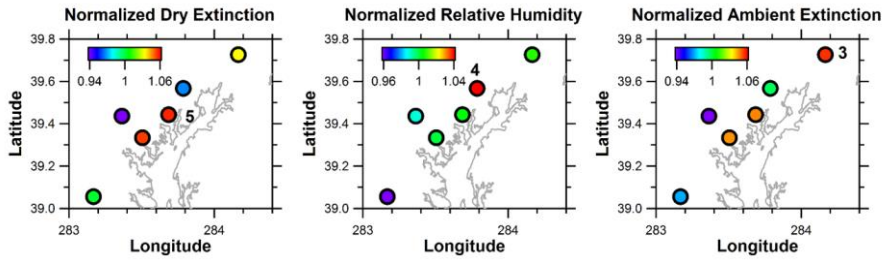
5
 6



	Slope	Y-Intercept
Baltimore	-0.42	0.60
Texas	-0.5	0.84
Western Pacific	-0.7	0.9
Northeast U.S.	-0.5	0.8
Indian Ocean	-0.3	0.5

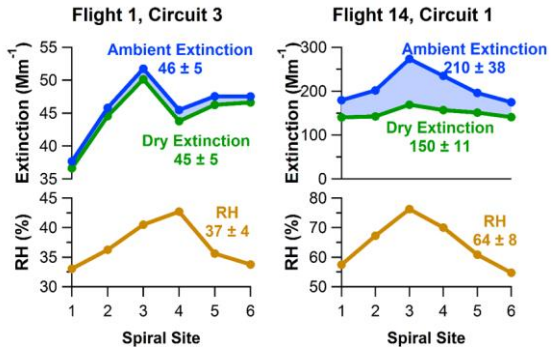
1
2
3
4
5
6
7
8
9

Figure 8. Relationship between γ (at 532 nm) and organic mass fraction for the present study (data below 1 km), Texas (Massoli et al., 2009), the western Pacific, the northeast U.S., and the Indian Ocean (Quinn et al., 2005). The organic mass fraction is found by dividing the WSOM by the total mass measured by the PILS and SP2. Other studies used organic mass measured by aerosol mass spectrometer or thermo-optical methods. The ratio of scattering at 80% RH to 20% [f(RH)] is shown on the right-axis (note the irregular spacing).



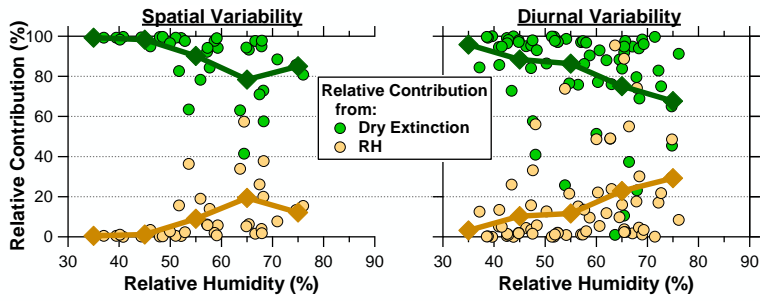
1
2
3
4
5
6
7

Figure 9. Average normalized 532 nm dry extinction (left panel), RH (center) and 532 nm ambient extinction (right) for all of the circuits (data is normalized to the average value for that circuit). The site with the maximum value is labelled.



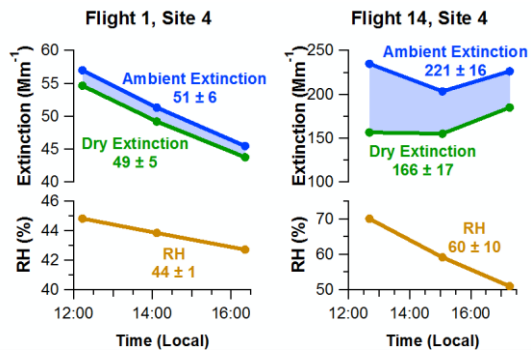
1
2
3
4
5

Figure 10. Average 532 nm ambient extinction, dry extinction and RH below 1 km during spirals over the six sites during Flights 1 and 14.



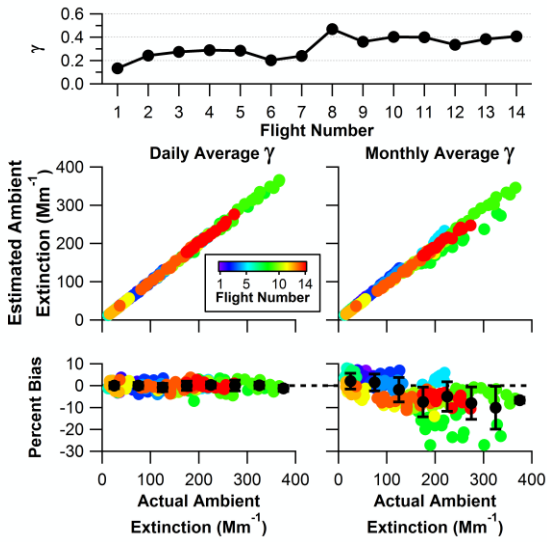
1
2
3
4
5
6

Figure 11. Relative contribution of dry extinction and RH on the spatial variability in ambient extinction as a function of RH (left) and on the diurnal variability (right). Diamonds represent the average relative contributions for 10% RH increments.

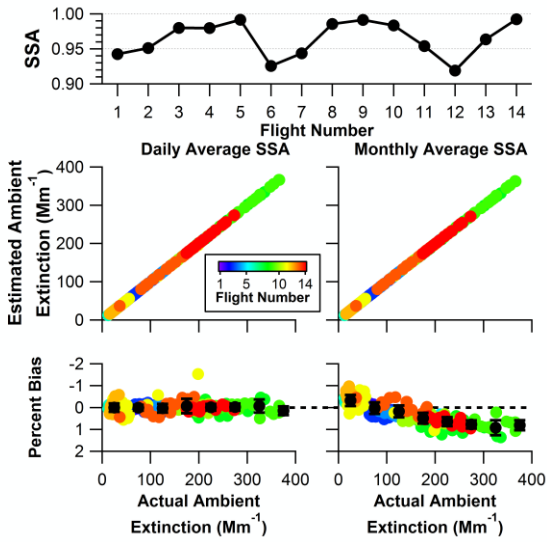


1
2
3
4
5

Figure 12. Trends in 532 nm ambient extinction, dry extinction and RH below 1 km during spirals at Site 4 during Flights 1 and 14.

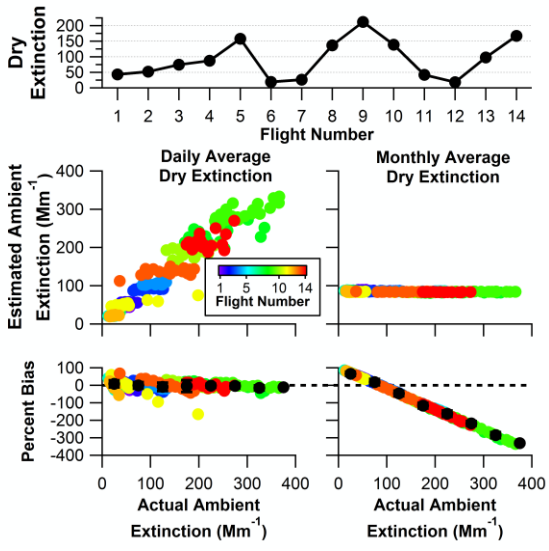


1
 2
 3 Figure 13. Average γ for each flight (top) along with estimated ambient extinction and percent
 4 bias if the flight-average (left) and campaign-average (right) γ are used.
 5



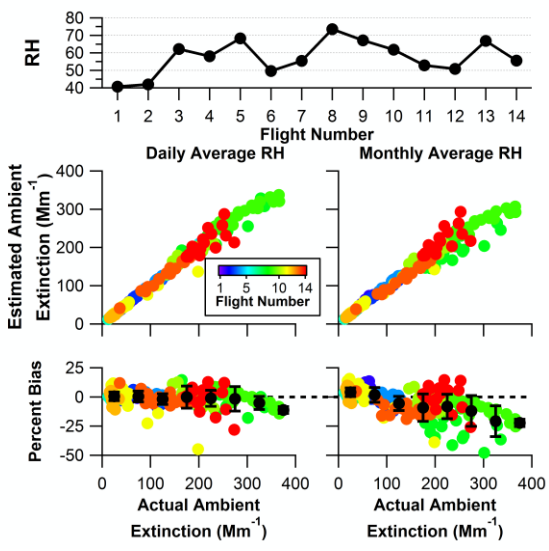
1
2
3
4
5

Figure 14. Average SSA for each flight (top) along with estimated ambient extinction and percent bias if the flight-average (left) and campaign-average (right) SSA are used.



1
2
3
4
5
6

Figure 15. Average dry extinction for each flight (top) along with estimated ambient extinction and percent bias if the flight-average (left) and campaign-average (right) dry extinction are used.



1
2

3 Figure 16. Average RH for each flight (top) along with estimated ambient extinction and
4 percent bias if the flight-average (left) and campaign-average (right) RH are used.